

THE HOLOCENE HISTORY OF NARES STRAIT

Transition from Glacial Bay to Arctic-Atlantic Throughflow

BY ANNE E. JENNINGS, CHRISTINA SHELDON, THOMAS M. CRONIN,
PIERRE FRANCUS, JOSEPH STONER, AND JOHN ANDREWS



Moderate Resolution Imaging Spectroradiometer (MODIS) image from August 2002 shows the summer thaw around Ellesmere Island, Canada (west), and Northwest Greenland (east). As summer progresses, the snow retreats from the coastlines, exposing the bare, rocky ground, and seasonal sea ice melts in fjords and inlets. Between the two landmasses, Nares Strait joins the Arctic Ocean (north) to Baffin Bay (south).
From http://visibleearth.nasa.gov/view_rec.php?id=3975

ABSTRACT. Retreat of glacier ice from Nares Strait and other straits in the Canadian Arctic Archipelago after the end of the last Ice Age initiated an important connection between the Arctic and the North Atlantic Oceans, allowing development of modern ocean circulation in Baffin Bay and the Labrador Sea. As low-salinity, nutrient-rich Arctic Water began to enter Baffin Bay, it contributed to the Baffin and Labrador currents flowing southward. This enhanced freshwater inflow must have influenced the sea ice regime and likely is responsible for poor calcium carbonate preservation that characterizes the Baffin Island margin today. Sedimentologic and paleoceanographic data from radiocarbon-dated core HLY03-05GC, Hall Basin, northern Nares Strait, document the timing and paleoenvironments surrounding the retreat of waning ice sheets from Nares Strait and opening of this connection between the Arctic Ocean and Baffin Bay. Hall Basin was deglaciated soon before 10,300 cal BP (calibrated years before present) and records ice-distal sedimentation in a glacial bay facing the Arctic Ocean until about 9,000 cal BP. Atlantic Water was present in Hall Basin during deglaciation, suggesting that it may have promoted ice retreat. A transitional unit with high ice-rafted debris content records the opening of Nares Strait at approximately 9,000 cal BP. High productivity in Hall Basin between 9,000 and 6,000 cal BP reflects reduced sea ice cover and duration as well as throughflow of nutrient-rich Pacific Water. The later Holocene is poorly resolved in the core, but slow sedimentation rates and heavier carbon isotope values support an interpretation of increased sea ice cover and decreased productivity during the Neoglacial period.

INTRODUCTION

The Arctic Ocean influences the global hydrological cycle by exporting freshwater and sea ice to the North Atlantic Ocean through Fram Strait and passages within the Canadian Arctic Archipelago (CAA), including Jones Sound, Lancaster Sound, and Nares Strait (Figure 1). Temporal and spatial variations in freshwater fluxes stabilize the water column and impede convective overturning, thereby influencing global thermohaline circulation (Aagaard and Carmack, 1989; Münchow et al., 2006; Goose et al., 2007). The freshwater and sea ice export through CAA straits is estimated to be responsible for only about 30% of total Arctic Ocean export, but modeling studies show that it can

have a major impact on convection in the Labrador Sea (Tang et al., 2004; Goosse et al., 2007).

There is strong geological evidence that Nares Strait was obstructed during the last glaciation by the coalescent Greenland and Innuitian Ice Sheets and was not deglaciated until the early Holocene (Blake, 1970; England, 1999; Zreda et al., 1999). The deglaciation of Nares Strait and the opening of a connection between the Arctic Ocean and Baffin Bay must have been a significant factor in the paleoceanographic development and paleoclimate history of Baffin Bay and the Labrador Sea. However, because of its remote and ice-covered location, few sediment cores have been collected that might document the opening of

Nares Strait and the subsequent evolution of Holocene environments. In August 2003, the scientific party aboard USCGC *Healy* collected a sediment core, HLY03-05GC, from Hall Basin, northern Nares Strait, as part of a study entitled “Variability and Forcing of Fluxes Through Nares Strait and Jones Sound: A Freshwater Emphasis” that was sponsored by the US National Science Foundation, Office of Polar Programs, Arctic Division (Falkner, 2003).

In this article, we investigate the timing of the opening of Nares Strait and the Holocene paleoceanographic developments during the deglaciation, the Holocene Optimum, and the Neoglacial cooling that followed through multiproxy analysis of HLY03-05GC (81°37.286'N, 63°15.467'W, 372 cm long, 797 m water depth; Figure 1). The paleoenvironmental reconstruction uses lithofacies descriptions and analysis, radiocarbon dating, benthic and planktic foraminiferal assemblages, and oxygen and carbon stable isotope analyses. Detailed analyses on this single, well-placed sediment core complement the aerially extensive terrestrial-based studies of glacial and sea ice history by providing a continuous, well-dated, Holocene marine record.

Environmental Setting

Nares Strait separates Ellesmere Island from Greenland and stretches from northern Baffin Bay to the Lincoln Sea, Arctic Ocean (Figure 1). The bedrock geology of the ice-free areas along Nares Strait is composed of Precambrian crystalline rocks overlain by Paleozoic platform carbonates (Funder, 1989; Parnell et al., 2007). This 530 km long

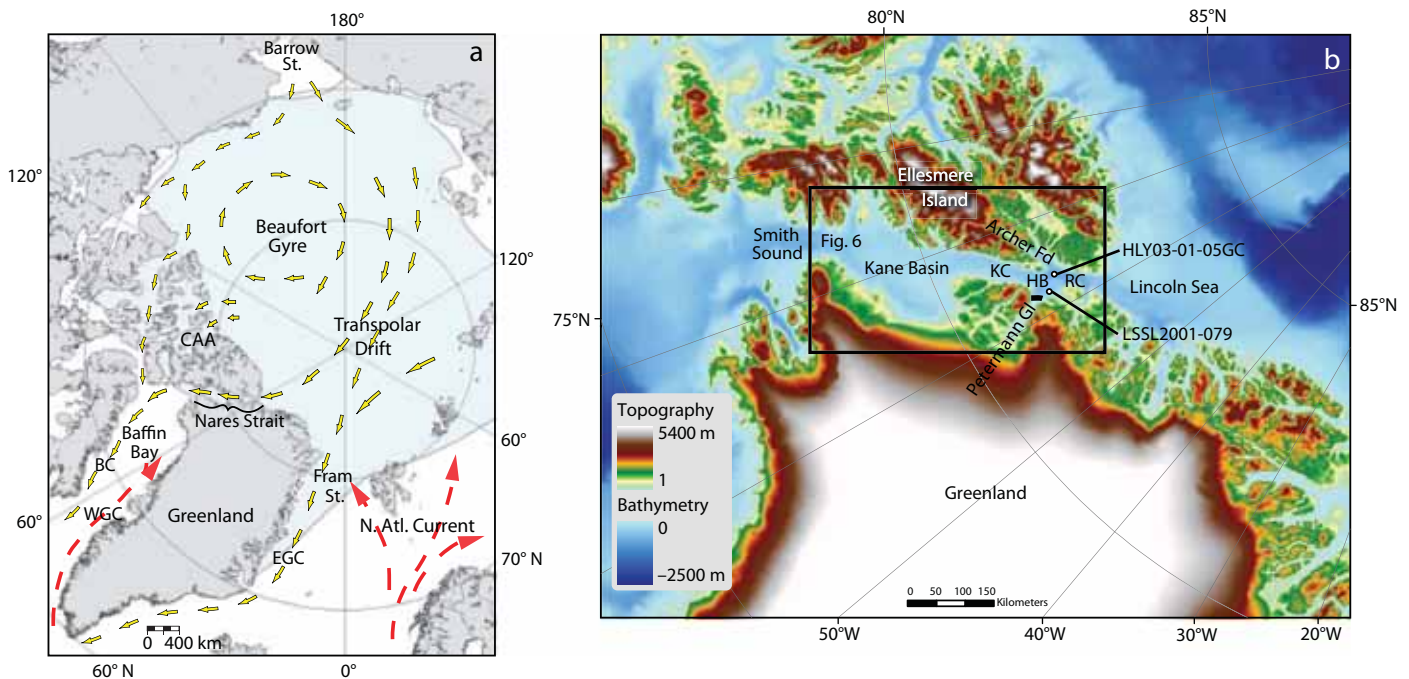


Figure 1. (a) Surface circulation in the Arctic Ocean showing summer sea ice (light blue), the pathway of Arctic Surface Water, made up largely of nutrient-rich, relatively low-salinity Pacific Water entering from Barrow Strait through Nares Strait, and of Atlantic Water entering the Arctic Ocean via Fram Strait and the Barents Sea. The Atlantic Water flows as a subsurface “Atlantic Layer” in the Arctic Ocean, entering Nares Strait beneath the Arctic Water. (b) Map showing details of Nares Strait physiography, the location of HLY03-05GC, the box that encloses Figure 6, the 450 m deep sill at the mouth of Petermann Glacier Fjord, and the location of core LSSL2001-079. RC = Robeson Channel. HB = Hall Basin. KC = Kennedy Channel. Bathymetric base map from IBCAO (Jakobsson et al., 2008).

channel is 40 km wide at its narrowest point, and 220 m deep at its shallowest sill in Kane Basin (Tang et al., 2004; Münchow et al., 2006). From north to south, Nares Strait is composed of Robeson Channel, Hall Basin, Kennedy Channel, Kane Basin, and Smith Sound (Figure 1). Hall Basin is an 800 m deep basin off Archer Fjord and Petermann Glacier Fjord, home of the Petermann Glacier, an outlet of the Greenland Ice

Sheet that terminates in a long, floating ice shelf. Petermann Fjord is over 1,000 m deep near the glacier front, but this deep basin lies behind a 350–450 m deep sill at the fjord mouth that separates the fjord from the deep Hall Basin (Figure 1b; Johnson et al., 2011).

Nares Strait is at least 80% covered by sea ice for 11 months of the year. Multiyear ice in the Arctic Ocean converges in the Lincoln Sea in mid

to late winter, forming an ice arch that completely blocks the flow of Arctic Ocean ice through Nares Strait (Kwok, 2005). Locally formed pack ice consolidates south of the ice arch and remains into the late summer, with the transition from landfast to drift ice usually occurring between mid-July and mid-August (Melling et al., 2001). Ice arches form at other constrictions along the strait, including Robeson Channel, Kennedy Channel, and Smith Sound (Samelson et al., 2006). They impede sea ice transit through the strait and promote the formation of the North Open Water polynya in northern Baffin Bay (Melling et al., 2001). The ice breaks out from south to north along Nares Strait. Sea ice can move at rates as high as 40 km per day (Kwok, 2005), driven by strong orographic and katabatic

Anne E. Jennings (anne.jennings@colorado.edu) is Research Scientist III, Institute of Arctic and Alpine Research (INSTAAR), and Associate Professor, Attendant Rank, Department of Geological Sciences, University of Colorado, Boulder, CO, USA. **Christina Sheldon** is a graduate student, Department of Geological Sciences, University of Colorado, Boulder, CO, USA. **Thomas M. Cronin** is a research geologist, US Geological Survey, Reston, VA, USA. **Pierre Francus** is Professor, Institut national de la recherche scientifique (INRS), Centre Eau Terre Environnement, Québec, Canada. **Joseph Stoner** is Associate Professor, College of Oceanic and Atmospheric Sciences, Oregon State University, Corvallis, OR, USA. **John Andrews** is Professor Emeritus, INSTAAR, University of Colorado, Boulder, CO, USA.

winds (Samelson et al., 2006). Water flows southward from the Arctic Ocean through Nares Strait into Baffin Bay driven by winds and the sea level drop along the length of the strait (Sadler, 1976; Münchow et al., 2006). The upper 100 m of the water column in Nares Strait is made up of low-salinity Arctic Water composed largely of nutrient-rich Pacific Water that enters the Arctic Ocean via Bering Strait, as well as freshwater from river runoff and sea ice melt (Münchow et al., 2007). Pacific Water has twice the nitrogen and phosphorus, and seven times the silica, of Atlantic Water, which fuels the high phytoplankton productivity of the Arctic shelves in surface water when sea ice cover retreats, thereby fueling benthic production. Arctic Water is underlain by Atlantic Water, which enters Nares Strait from the Arctic Ocean and can have its source in either the Barents Sea or the Fram Strait branches of the Norwegian Atlantic Current (Figure 1; Jones et al., 2003; Münchow et al., 2006). Arctic Water flows southward through Nares Strait, but the strait is too shallow in places to allow Atlantic Water to flow through. Atlantic Water in Smith Sound at the southern end of Nares Strait is derived from the West Greenland Current.

Arctic Water entering Baffin Bay through Nares Strait is incorporated into the southward flowing Baffin Current and continues to the Labrador Sea where variations in its flux have been related to variability of deep convection in the Labrador Sea (Figure 1; Tang et al., 1999; Goosse et al., 2007). The Arctic outflow through CAA has a high content of nutrient-rich Pacific waters, which have a low saturation state with respect to calcite, resulting in poor

preservation of CaCO_3 microfossils and molluscs on its path along the Baffin Island shelf southward along Labrador (Azetsu-Scott et al., 2010).

Glacial History

Study of HLY03-05GC is framed by glacial geological reconstructions for CAA (Blake, 1970; England, 1999; Dyke et al., 2002; England et al., 2006) and northern Greenland (Kelly and Bennike, 1992; Larsen et al., 2010; Möller et al., 2010; Funder et al., in press). The Greenland Ice Sheet (GIS) advanced to fill Nares Strait after 19,000 ^{14}C yrs BP during the Kap Fulford stade (cold interval; Kelly and Bennike, 1992), allowing the Innuitian Ice Sheet (IIS) to thicken and achieve maximum growth

confluent ice flowing from Nares Strait into the Lincoln Sea (Funder et al., in press). Heavy sea ice cover in the Arctic Ocean is thought to have deflected the shelf-based ice eastward along the north coast of Greenland (Larsen et al., 2010). Minimal inflow of Atlantic Water beneath a thick halocline would have shielded the shelf-based ice (Larsen et al., 2010). The shelf-based ice is thought to have receded between 16,000 cal BP and 10,300 cal BP. The Greenland Ice Sheet margin had retreated to the fjord mouths of Northwest Greenland by 11,200 cal BP, with final breakup close to 10,100 cal BP marked by a marine transgression (Larsen et al., 2010; Funder et al., in press).

Between 8,000 and 7,500 ^{14}C yrs BP,

“ RETREAT OF GLACIER ICE FROM NARES STRAIT AND OTHER STRAITS IN THE CANADIAN ARCTIC ARCHIPELAGO AFTER THE END OF THE LAST ICE AGE INITIATED AN IMPORTANT CONNECTION BETWEEN THE ARCTIC AND THE NORTH ATLANTIC OCEANS, ALLOWING DEVELOPMENT OF MODERN OCEAN CIRCULATION IN BAFFIN BAY AND THE LABRADOR SEA. ”

late in the Last Glacial Maximum (England, 1999). The glacier ice flowed northward from a divide in Kane Basin and advanced into the Lincoln Sea. On northernmost Greenland, Larsen et al. (2010) and Möller et al. (2010) reconstruct a shelf-based ice sheet that flowed eastward along the coastal plain with at least one source being the

the connection between GIS and IIS was severed and Nares Strait became an open conduit between the Arctic Ocean and Baffin Bay. Postglacial marine limits on the Greenland side of Nares Strait are greatest (up to 130 m) in the land area adjacent to Hall Basin and Petermann Glacier (Funder and Hansen, 1996). Along most of the length of Nares Strait,

relative sea level was 80 to 120 m higher than present in the early Holocene in response to retreat of the ice sheet and unloading of the crust (Funder and Hansen, 1996; England et al., 2006). As a result, water depths along Nares Strait and at the entrance to the Arctic Ocean were considerably deeper in the early Holocene than they are today.

One other marine sediment core has been taken in the area. LSSL2001-079 PC consists of 8 m of calcareous mud (Figure 1). Radiocarbon dates in this core formed age reversals, and a radiocarbon date of $14,070 \pm 100$ ^{14}C yrs BP in stratified sediments was interpreted to indicate that Hall Basin had not been inundated by grounded ice for at least 16,800 cal years (Mudie et al. 2006). It is unclear what material was dated and whether there was a source of old carbon to produce this date. In any event, the interpretation of the “old” date in LSSL2001-079PC conflicts with the glacial history presented from terrestrial glacial records (England, 1999; Kelly and Bennike, 1992) and data presented in this paper.

MATERIALS AND METHODS

The site for collection of HLY03-05GC was chosen on the basis of acoustic profiles and swath bathymetry. SeaBeam high-resolution swath bathymetry showed a northeast-to-southwest-trending U-shaped channel exceeding 800 m water depth forming the western side of Hall Basin. The 3.5-kHz Bathym2000 data revealed a 30 m thick section consisting of two acoustic units: an upper, horizontal, transparent surface layer 5–10 m thick overlying a 25 m thick unit with multiple parallel acoustic reflectors (Falkner, 2003). The 371 cm long HLY03-05GC core was recovered

from 81°37.286'N and 63°15.467'W on August 11, 2003 (Figure 1), at 797 m water depth. We were unable to access the 3.5 kHz record from the site, but it is likely that the core lies fully within the upper transparent acoustic unit.

Lithofacies

Lithofacies descriptions are based on visual core descriptions and photographs of newly split cores, x-radiography, and computerized tomographic (CT) scanning. Visual core descriptions were made a year after collection at the Oregon State University (OSU) core repository where the core is archived. Digital x-radiographs were taken of the working half of the core prior to sampling in 2008 at the veterinary hospital on the OSU campus. CT density measurements were performed on the archive half of the core at the Oregon State University College of Veterinary Medicine in 2010 using a Toshiba Aquilion 64 Slice. Scans were collected at 120 kVp and 200 mAs. For visualization purposes, the resulting images were processed with a “sharp” algorithm to generate sagittal and coronal images every 4 mm across the core. Down-core and across-core pixel resolution within each slice is 500 μm . The cores were scanned in ~ 60 cm segments and then joined into a composite image using Adobe Photoshop software.

In order to study the origin of the laminations, thin sections were sampled, using the technique described in Francus and Asikainen (2001), from three intervals: (a) 104.5–122.5 cm, (b) 146.5–164.8 cm, and (c) 240.5–258.9 cm (Figure 2). Thin sections were prepared using a freeze-drying technique and were observed

on petrographic and scanning electron microscopes. Micro-x-ray fluorescence (XRF) scans made on each of the thin section blocks yielded chemical content with a resolution of 100 μm in the direction perpendicular to the stratigraphy (e.g., Cuven et al., 2010).

Chronology, Radiocarbon Dating

Seven radiocarbon dates were obtained: five were on the polar planktonic foraminifer, *Neogloboquadrina pachyderma* sinistral (NPS), the top date was from an individual mollusk, and the basal date was from a combination of NPS and the benthic foraminifer *Cassidulina neoteretis* (Table 1). We present calibrated ages and ^{14}C ages using a 400-year ocean reservoir correction (i.e., $\text{DR}=0$) for all samples and boundaries within the core in order to make the clearest comparison with the published glacial history concerning the Innuitian Ice Sheet, which is reported in ^{14}C years corrected for an ocean reservoir age of 400 or 410 years ($R = 400$ or 410 yrs). We recognize that a larger ocean reservoir correction likely is needed for some of the ^{14}C dates on marine carbonates from the Canadian Arctic Archipelago. A large ocean reservoir age of 735 ± 85 yrs has been carefully determined (Dyke et al., 2003; Coulthard et al., 2010), so Table 1 also shows the HLY03-05GC calibrated ages for this larger DR in order to envelop the probable high and low calibrated ages. To complicate this issue further, researchers on northern Greenland use an ocean reservoir age of $R = 550$ (i.e., $\text{DR} = 150$ yrs) to calibrate the North Greenland glacial records (Larsen et al., 2010; Möller et al., 2010; Funder et al., in press). We calibrated the radiocarbon dates from HLY03-05GC

using Calib 6.0 (Stuiver et al., 2010) with the Marine09 calibration curve (Reimer et al., 2009; Table 1). The HLY03-05GC record extends from 160 to 10,300 cal BP (130–9,010 ^{14}C yrs BP). The age model for the core is a 0-weight curve fit between the dated levels (Figure 2).

Benthic and Planktic Foraminiferal Assemblages

Foraminiferal subsamples were 2 cm wide and were taken every 10 cm for the length of the core. Samples were freeze-dried, weighed, soaked in distilled water and sodium metaphosphate, then wet sieved at 1000 μm , 106 μm , and 63 μm . The sieve fractions were air dried and weighed, and these sieve fractions provide grain size information (Figure 2).

Benthic and planktic foraminiferal species were identified in the 1,000–106 μm fraction using a binocular microscope. Where possible, at least 200 specimens were picked from each sample, to obtain a representative assemblage at each depth. For most samples, a microsplitter was used to obtain a representative fraction. However, below 125 cm, there were several samples whose entire count was below 200. All specimens were identified to genus and species level.

The assemblages of foraminiferal species provide key information about the water masses present in Hall Basin (Atlantic Water, Arctic Water, glacial meltwater), marine productivity (controlled by nutrients in the water, the duration of sea ice cover), sedimentation rates, and the basic physiography of Hall Basin (i.e., is it a deep basin in front of an ice margin facing the Arctic Ocean shelf or is it a basin within a through flowing strait?).

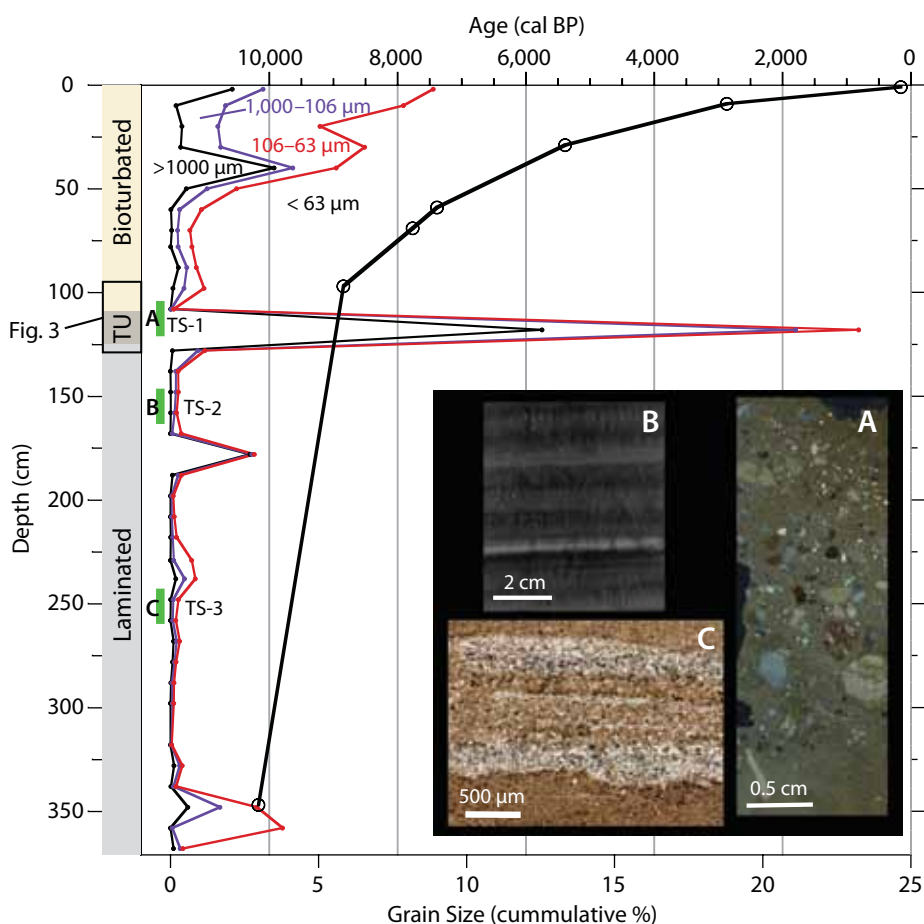


Figure 2. Grain-size variations and the calibrated age model for HLY03-05GC shown against depth and lithofacies. The vertical green bars on the core log show the intervals where thin sections were made (TS-1, -2, and -3). (Inset A) Cross-polarized image of the thin section from 119.6 to 122.6 cm in the transitional unit (TU) viewed under a light microscope, showing abundant ice-rafted debris (IRD). (Inset B) CT scan image of vertical burrows in the upper, more bioturbated part of the laminated mud from 155–161 cm. (Inset C) Light microscope image from thin section C from 253–253.5 cm that illustrates two coarse laminations. The erosive base (wavy basal contact) and normal grading in the coarse laminations support an interpretation of turbidity current deposition. The box around the transitional unit shows the depth interval represented in Figure 3.

Stable Isotope Analyses

Stable isotopes of oxygen and carbon were measured on tests (shells) of benthic *C. neoteretis* and planktic *Neogloboquadrina pachyderma* sinistral (NPS) foraminifers at the Woods Hole Oceanographic Institution Mass Spectrometer Facility. $\delta^{18}\text{O}$ values were corrected for sea level changes using Fairbanks' (1989) data. Twenty specimens with diameters between 150 and 250 μm

of each species were submitted for analysis. The $\delta^{18}\text{O}$ values of foraminiferal tests vary with both the temperature and isotopic composition of the ocean water in which the foraminifers calcify. Lighter $\delta^{18}\text{O}$ values reflect fresher and/or warmer water, and heavier $\delta^{18}\text{O}$ values indicate colder and/or saltier water. Very light values can result from influx of isotopically light glacial meltwater. Surface water productivity and export to the seafloor

of isotopically light organic matter produced in the surface water are the main controls on $\delta^{13}\text{C}$ values in the foraminifers, with large differences in benthic and planktic $\delta^{13}\text{C}$ values pointing to higher productivity and efficient export of labile organic matter to the seabed (Maslin and Swann, 2005). An additional factor for the $\delta^{13}\text{C}$ values of benthic foraminifers is the “Mackensen effect” (Mackensen et al., 1993) in which growth and reproduction of benthic foraminifers, such as *C. neoteretis*, coincide with the episodic production of isotopically light phytodetritus (plant matter formed in the surface ocean that rains onto the seafloor); the effect is isotopically light $\delta^{13}\text{C}$ tests, which reflect episodic productivity. Episodic seasonal productivity is characteristic of sea ice-dominated environments with short open-water seasons, such as Nares Strait.

RESULTS
Sedimentological Proxies

X-radiography, photographs, and CT scans of HLY03-05GC reveal two main sediment lithofacies: laminated mud and bioturbated mud, and an intervening

transitional unit containing pebble-sized iceberg-rafted stones (ice-rafted debris, or IRD; Figure 2). The substantial sedimentological changes associated with the lithofacies reflect major Holocene paleoenvironmental changes.

Laminated Mud
(125–371 cm, 8,990–10,300 cal BP)

This early Holocene unit is visually laminated by color and grain size, with color variations between dark gray (5Y4/1) and dark grayish brown (2.5Y4/2) (Figure 2). This unit is rapidly deposited relative to the upper unit, with an average sedimentation rate of 0.19 cm yr⁻¹ or 5.3 yrs cm⁻¹ (Figure 2). Although detailed grain-size measurements were not made, the thin sections and CT scans clearly illustrate grain size variations associated with the laminations. The coarser layers have a brown hue and are 1–2 mm thick in general. Normal grading is visible in the few coarse layers that are up to 3 cm thick. The finer components of the laminations are dark gray. On average, the visual laminations are 0.5 cm thick. The CT scans reveal bioturbation throughout

the laminated mud. The bioturbation is most common in the less-dense (finer) laminations. Individual burrows tend to be abruptly terminated by the denser (coarser) layers. From 213 cm (8,370 ¹⁴C yrs BP, 9,460 cal BP) to the top of the unit, bioturbation becomes more pervasive. Vertical burrows in the low-density fine units are clearly terminated by overlying coarser units (Figure 2B). Vertical burrows signify rapid sedimentation; burrow termination by coarser layers suggests episodic sedimentation. The thin section from 252.8 to 258.9 cm demonstrates sharp, wavy basal contacts on the coarser laminations indicative of erosion (Figure 2C). Rare flame structures and cross cutting of coarse laminae by overlying laminae were observed on the CT scan and the x-radiographs. These characteristics support episodic, low-concentration turbidity current deposition in Hall Basin as the origin for the laminated unit (Pickering et al., 1986; Ó Cofaigh and Dowdeswell, 2001), which is consistent with distal glacial marine sedimentation (Syvitski and Hein, 1991). The uniform elemental composition shown by micro XRF data

Table 1. Radiocarbon dates from core HLY03-05GC, Hall Basin, northern Nares Strait.

Sample Depth in Core (cm)	Laboratory Number	Reported ¹⁴ C Age	$\delta^{13}\text{C}$	$\Delta R = 400 \pm 0$ Cal BP Range (1 σ)	Median Probability Age (yrs BP)	$\Delta R = 335 \pm 85$ Cal BP Range (1 σ)	Median Probability Age (yrs BP)	Material Dated	Mass (mg)
0–2	AA-81309	530 \pm 52	2.4	99–249	159	na	na	<i>Batharca glacialis</i>	3.2
8–10	NOS-71686	3,100 \pm 35	0.75	2,817–2,927	2,872	2,357–2,609	2,501	NPS	11.4
2–30	NOS-71687	5,040 \pm 40	0.66	5,326–5,437	5,388	4,817–5,072	4,961	NPS	15.2
58–60	NOS-71688	6,870 \pm 45	0.44	7,333–7,425	7,385	6,929–7,159	7,044	NPS	5.5
68–70	AA-81310	7,302 \pm 61	0	7,690–7,829	7,766	7,386–7,566	7,468	NPS	11.4
96–98	NOS-72574	8,290 \pm 50	0.01	8,769–8,951	8,846	8,328–8,528	8,424	NPS	5.6
345–349	NOS-71689	9,320 \pm 45	0.23	10,135–10,215	10,171	9,528–9,798	9,686	NPS & <i>C. neoteretis</i>	4.5

All calibrations with DR = 400 \pm 0 and DR = 735 \pm 85 (Coulthard et al., 2010) and Marine09 calibration (Hughen et al., 2004; Reimer et al., 2009). na = not available; NPS = *Neogloboquadrina pachyderma* sinistral

in this thin section suggests a consistent and limited sediment source area over this interval. Grain size drives the only significant variability; the coarse laminations are enriched in Zr and Ca, probably reflecting a source in the Paleozoic carbonate bedrock (Parnell et al., 2007).

Transitional Unit

(112–125 cm, 8,930–8,990 cal BP)

The transitional unit is laminated in its lower part (125–118 cm) and heavily bioturbated, with only faint evidence of lamination remaining in its upper part (118–112 cm). The increase in granule to pebble-sized grains characterizes this 13 cm long unit (Figures 2 and 3). Thin section analyses show dispersed, faceted clasts and till pellets floating in a finer matrix (Figure 2A). These clasts are interpreted to reflect sediment released from icebergs (IRD). In the lower, laminated part of the transitional unit, IRD is concentrated in the coarser layers. In the upper, bioturbated part of the transitional unit (118–112 cm), the outsized clasts are dispersed. Variable elemental compositions in this interval suggest diverse sediment sources for the material. The Transitional Unit is interpreted to represent the opening of Nares Strait by final breaching of the Greenland Ice Sheet from the shallow Kennedy Channel (England, 1999).

Bioturbated Mud

(0–112 cm, 160–8,930 cal BP)

This unit is essentially devoid of laminations except for the basal interval from 112–107 cm in which some residual stratification is visible in the CT scan (Figure 2). The whole interval is thoroughly bioturbated (Figure 2). There are two main burrow types: numerous,

small, sinuous burrows of millimeter scale, and fewer, larger, (1 cm diameter and up to 5 cm long) horizontal burrows. IRD (> 1 mm clasts) is very rare to absent from 112–70 cm, but becomes more abundant in the upper 50 cm of the core (Figure 2). Sedimentation rates decline from 0.026 to 0.003 cm yr⁻¹ over this unit (Figure 2). The pervasive bioturbation reflects sufficient primary productivity to support the benthic community and slower sedimentation rates (Wetzel, 1991). The horizontal burrows are consistent with the slow sedimentation rates. Elemental analysis of the thin section from 104.5–112.5 cm shows inverse correlation between

iron and calcium, which may reflect the increasing quantities of calcareous foraminifers and decreasing products of glacial erosion associated with the bioturbated mud (Figure 4).

Paleoceanographic Proxies

Foraminifera

The Arctic species *Neogloboquadrina pachyderma* sinistral (NPS) is the only planktic species present. Arctic assemblages usually are dominated (≥ 95%) by NPS, although subpolar or ocean front species have been found in the Arctic Ocean in sediments of much older interstadial and interglacial intervals and have been used to infer diminished summer

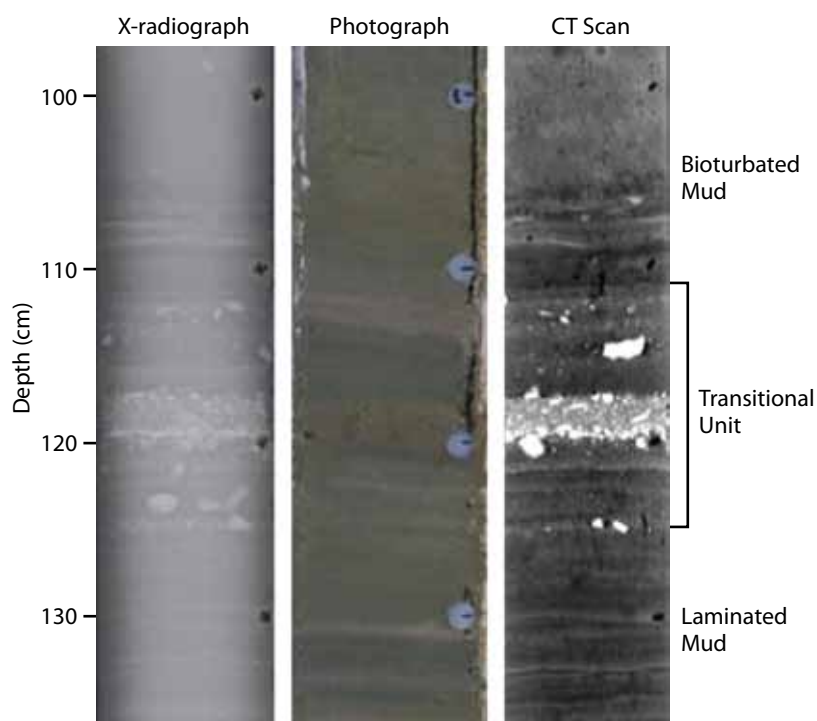


Figure 3. Comparison of x-radiography, photography, and CT scan of the transition from laminated mud to bioturbated mud in HLY03-05GC. The transitional unit is interpreted to manifest the opening of Nares Strait, changing Hall Basin from a glacial bay facing the Arctic Ocean to an open connection between the Arctic Ocean and Baffin Bay. The x-radiograph is from the working half of the core while the photograph and CT scan are from the archive half, so the x-radiograph has some differences in ice-rafted clasts.

sea ice (Adler et al., 2009).

The numbers of benthic and planktic foraminifers per gram are both very low in the laminated and transitional units and rise dramatically in the bioturbated mud (Figure 4). However, this change can be ascribed largely to the decrease in sedimentation rates of nearly two orders of magnitude. The benthic to planktic foraminiferal ratio is much higher in the laminated mud than in the bioturbated mud, indicating that the bioturbated mud is more “oceanic.” *Cassidulina neoteretis*, which makes up as much as 90% of the benthic fauna, dominates the entire record. High percentages of *Cassidulina neoteretis* are common in the relatively warm and saline

“Atlantic Layer” of the Arctic Ocean (~ 500–1,100 m) that derives from cooled Atlantic Water, forming a subsurface water mass beneath fresher, colder Arctic Water (Jennings and Helgadottir, 1994; Osterman et al., 1999; Rytter et al., 2002; Jennings et al., 2004). The entire record is strongly influenced by the presence of subsurface Atlantic Water.

Although *C. neoteretis* dominates the core, there are large faunal changes that coincide with lithofacies changes and provide clues about the progression of environmental change through time (Figure 4). In the laminated mud, *Cassidulina reniforme* co-dominates with *C. neoteretis*, with subsidiary percentages of *Stainforthia concava* and *Elphidium*

excavatum forma *clavata*. The species in the laminated mud are consistent with cold, ice-distal glaciomarine conditions, just as was determined from the sedimentological proxies. However, entry of *Oridorsalis umbonatus* and *Miliolinella subrotunda* in the upper part of laminated mud and through the transitional unit and the increase in bioturbation by 213 cm indicate diminishing influence of retreating and/or thinning glacier ice. *Oridorsalis umbonatus* occupies a depth habitat in the Arctic Ocean between 1,100 and 3,500 m water depth (Osterman et al., 1999). This slope-dwelling species is adapted to low food supply. Its presence in Hall Basin is consistent with glacioisostatic deepening of the entrance to Arctic Ocean north of Hall Basin, which may have been as much as 130 m deeper (England et al., 2006). *Miliolinella subrotunda* is a benthic species adapted to episodic productivity. Its presence beginning in the upper part of the laminated unit, where bioturbation becomes more pronounced, supports periods of marine productivity that would require some open water. The fauna in the laminated mud and the transitional unit reflect a progression to less glacially influenced environments and increased water depths due to glacioisostatic depression, ending with the transition to an open strait at the end of glaciomarine conditions.

The fauna changes dramatically in the bioturbated mud. *C. reniforme* is replaced by *Nonionellina iridea*, a species that feeds on phytodetritus produced episodically at the sea surface and deposited on the seabed as labile organic matter (Gooday and Hughes, 2002). It occurs in the earliest part of

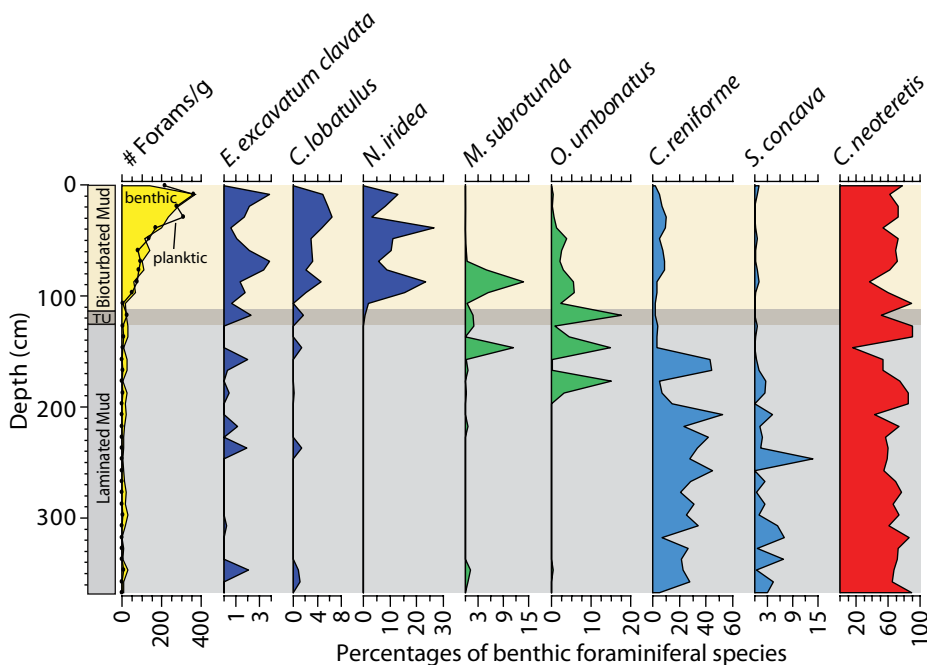


Figure 4. Benthic and planktic foram abundances (numbers per gram) and the percentages of key species in the benthic foraminiferal assemblages of HLY03-05GC shown against the lithofacies and depth in the core. Colors highlight the dominant species in the stratigraphic succession: Light blue = glacial marine species in the laminated mud. Green = Arctic species in the transition Dark blue = species in the bioturbated mud. Red = Atlantic Intermediate Water indicator *C. neoteretis*, which dominates the assemblage throughout the record. The assemblages indicate distal glacial marine condition in the laminated mud and intervals of high marine productivity in the bioturbated mud. *Oridorsalis umbonatus* entering the assemblage in the upper part of the laminated mud likely indicates a deeper connection to the Arctic Ocean by glacioisostatic loading.

the bioturbated mud with *Miliolinella subrotunda*, which also is known to take advantage of productivity spikes (Altenbach et al., 1993). The presence of these species is consistent with a longer open sea ice season relative to the laminated unit. Marine productivity changes can follow the sea ice margins where large, episodic phytodetritus blooms deliver high food fluxes to the seabed (Steinsund, 1994; Polyak et al., 2002; Rytter et al., 2002), or where the duration of the sea ice free season is lengthened in response to warming, allowing more productivity at the sea surface and rapid delivery of organic matter to the seabed. Marine productivity also would have been affected by passage of nutrient-rich Pacific sourced Arctic Water that began to flow through the strait on deglaciation.

Cibicides lobatulus is also present in the bioturbated mud. This sessile epibenthic (living attached on the seabed) species reflects strong currents, and its tests probably were washed into Hall Basin from the shallower margins of Nares Strait after death by increased current activity associated with the opening of the strait. The abundance of *Elphidium excavatum* forma *clavata* is inversely correlated with that of *N. turgida*. *E. excavatum clavata* tolerates lowered salinities and harsh conditions (Hald et al., 1994; Hald and Korsun, 1997).

Stable Isotopes

The benthic oxygen isotopes are heavy throughout the laminated unit, suggesting consistently cold, saline bottom water conditions (Figure 5). $\delta^{18}\text{O}$ *C. neoteretis* values lighten abruptly right above the transitional unit by 0.4‰,

which would represent almost 2°C warming were it related solely to temperature. Subsequent values fall abruptly by 0.2‰ to 3.7‰ and trend in general to heavier values thereafter, which may reflect cooling. The planktic $\delta^{18}\text{O}$ is much more variable, spiking to very light values (2–2.1‰) throughout the laminated mud, but especially in the least-bioturbated interval below 213 cm. These depleted spikes likely reflect isotopically light glacial meltwater (Figure 5). A final light spike in planktic $\delta^{18}\text{O}$ occurs near the top of the laminated unit, closely preceding the transitional unit.

Benthic $\delta^{13}\text{C}$ shows typical Atlantic

Water values larger than 0‰ in the laminated mud and heavy $\delta^{18}\text{O}$ values, suggesting cold bottom water conditions (Figure 5). A 0.5‰ $\delta^{13}\text{C}$ lightening begins in the transitional unit (8,950 cal BP) and deepens in the bioturbated mud, persisting to 39 cm (6,050 cal BP). This lightening is consistent with increased phytodetritus flux to the seabed, leading to $\delta^{13}\text{C}$ depleted pore waters. Increased productivity and export of organic matter parallels the increase in the productivity indicator species *N. iridea*. Such a shift can be explained by throughflow of high-nutrient Pacific Water and

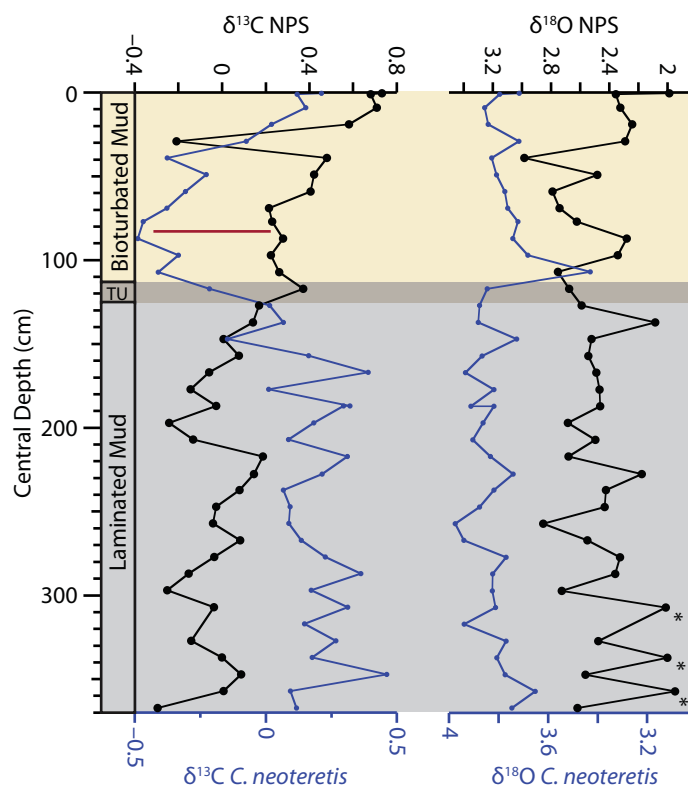


Figure 5. Paleoceanographic proxies in benthic (*Cassidulina neoteretis*) and planktic (*Neogloboquadrina pachyderma sinistral* = NPS) foraminifers. The $\delta^{18}\text{O}$ data are corrected for sea level change according to Fairbanks' (1989) data. The $\delta^{13}\text{C}$ differences between benthic and planktic foraminifers are large (red line) in the bioturbated mud, indicating high productivity and export of labile organic carbon from the surface ocean to the seabed. The asterisks on the $\delta^{18}\text{O}$ NPS plot indicate isotopically light intervals that likely reflect glacial meltwater.

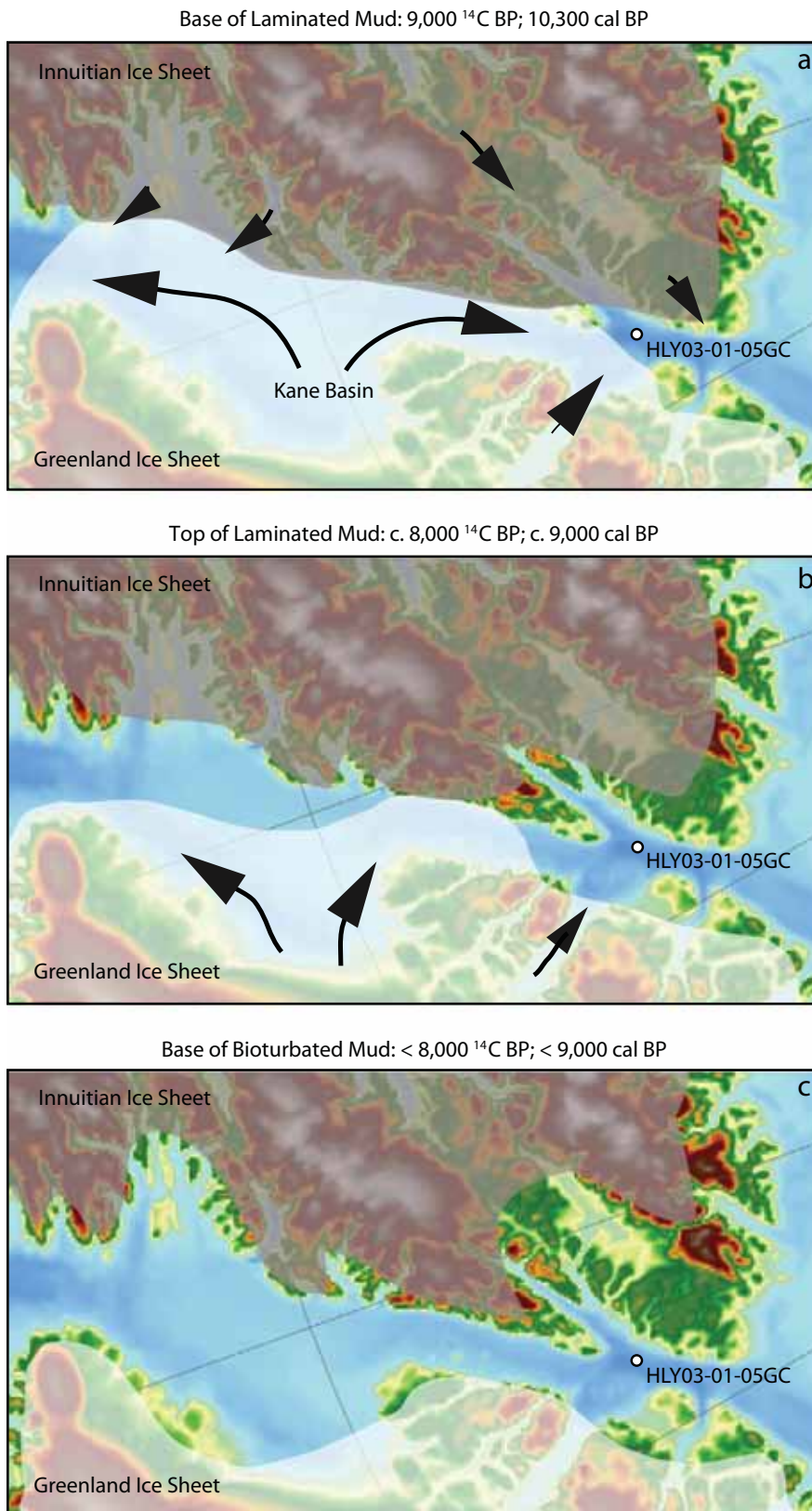


Figure 6. Schematic maps modified from England (1999) with additional insight from Kelly and Bennike (1992) and Funder et al. (in press) showing proposed configurations of the Innuitian (gray overlay) and Greenland (white overlay) Ice Sheets as manifested in the lithofacies changes of HLY03-05GC.

diminished sea ice cover. The benthic $\delta^{18}\text{O}$ values spike up by 0.4‰ at the base of the bioturbated mud, either indicating warming or freshening of the bottom water at the opening of the strait.

DISCUSSION

Timing and Environments of Ice Sheet Retreat

We present schematic maps modified from England (1999) showing the configuration of GIS and IIS at three critical times during the deposition of HLY03-05GC (Figure 6). The laminated mud represents distal glacial marine sedimentation in an embayment or glacial bay facing the Arctic Ocean (Figure 6a). The presence of distal glacial marine sediments means that the deep Hall Basin was deglaciated prior to 9,020 ¹⁴C yrs BP (= 10,300 cal BP). Based on observations in the HLY03 cruise report (Falkner et al., 2003), there are 25 m of acoustically stratified sediments below the basal sediments of HLY03-05GC. These sediments represent much more ice-proximal glaciomarine sediments deposited rapidly as the Greenland Ice Sheet margin was retreating from Hall Basin. The good match between the timing of distal glaciomarine sedimentation in Hall Basin and the breakup of shelf-based ice off northern Greenland (Larsen et al., 2010; Möller et al., 2010) demands rapid sedimentation of the stratified “ice-proximal” unit. The shelf-based ice likely is a northward and eastward extension of a confluent Greenland and Innuitian Ice Sheet outlet flowing north out of Nares Strait (Funder et al., in press).

Based upon radiocarbon ages on molluscs calibrated with an ocean reservoir of 550 years (i.e., 100 to 200 years younger than those calibrated with

an ocean reservoir of 400 years), the shelf-based ice off North Greenland broke up close to 10,100 cal BP (Larsen et al., 2010). The 10,300 cal BP basal age of HLY03-05GC matches well with the timing of the breakup of the shelf-based ice and continued retreat of the

In support of the Atlantic Water hypothesis, the HLY03-05GC data suggest that the Atlantic Layer was present in Hall Basin throughout the period of deglaciation, and it likely assisted rapid melting of the marine-based ice outlet (cf. Holland et al., 2008).

Petermann Glacier had already retreated from Hall Basin and thus conflicts with an extended Petermann Glacier lobe overlying the core site. We suggest that the ice margin had retreated out of the deep Hall Basin to a pinning point of the shallower sill at the mouth of Petermann Fjord (Johnson et al., 2011) by this time, but we do not currently have an alternative explanation for the formation and timing of the Cape Baird foreset beds.

“...GIVEN THE ADVANCES IN TECHNIQUES FOR STUDYING PALEOCEANOGRAPHY SINCE THE 1980s, IT SHOULD BE POSSIBLE, WITH NEW CORES, TO GAIN A BETTER UNDERSTANDING OF HOW THE OPENING OF A CONNECTION WITH THE ARCTIC OCEAN AFFECTED THE PALEOCEANOGRAPHIC DEVELOPMENT OF BAFFIN BAY AND THE LABRADOR SEA.”

ice margin into Hall Basin. England (1999) shows marine embayments formed by ice retreat, initiated on the north and south ends of Nares Strait by 9,000 ^{14}C yrs BP (10,240 cal BP), suggesting an excellent fit among the data sets. However, the HLY03-05GC glacial marine sediments indicate that the marine embayment was at least 50 km larger, and probably included all of Hall Basin at 9,000 ^{14}C yrs BP (10,300 cal BP). The rapid ice retreat and expansion of a marine embayment have been attributed to increased inflow of Atlantic Water (Andrews and Dunhill, 2004; Larsen et al., 2010; Möller et al., 2010), a thinner Arctic Ocean halocline (Jakobsson et al., 2010), and orbital forcing of higher summer temperatures (Berger and Loutre, 1991).

An inconsistency arises between the terrestrial-based reconstruction (England, 1999) and the HLY03-05GC data at 8,500 ^{14}C yrs BP, when a lobe of the Petermann Glacier is reconstructed to extend into Hall Basin over the HLY03-05GC site and terminate in the deep water. A shell date of 8,400 ^{14}C yrs BP (equivalent to 9,480 cal BP) in ice-contact delta foreset beds that dip toward Ellesmere Island on the northern tip of Judge Daly Promontory supports extension of the Petermann Glacier to a pinning point on the Judge Daly Promontory at that time (England, 1999). However, the presence of distal glaciomarine sediments in HLY03-05GC with a ^{14}C date on foraminifers of 8,920 ^{14}C yrs BP (9,700 cal BP) indicates that the

Opening of Nares Strait (7,952–8,005 ^{14}C yrs BP, 8,926–8,994 cal BP)

Multiple lines of evidence support the interpretation that the transitional unit represents retreat of the Greenland Ice Sheet from Kennedy Channel and the transition from a glacial bay to an open connection between the Arctic Ocean and Baffin Bay at 8,005 ^{14}C yrs BP, 8,565 cal BP (Figure 6b,c). The age model indicates that the transition is short-lived, ending by 7,950 ^{14}C yrs BP, 8,930 cal BP. According to the glacial reconstruction of England (1999) and England et al. (2006), the strait was still closed at 8,000 ^{14}C yrs BP, but the opening was established by 7,500 ^{14}C yrs BP. Considering the vastly different data sets, this age comparison is quite close.

Changes in Sea Ice Cover and Marine Productivity: Holocene Climatic Optimum to Neoglacial Cooling

The bioturbated mud clearly represents sedimentation in a strait that formed a connection between the Arctic Ocean and Baffin Bay close to 8,000 ^{14}C yrs BP (9,000 cal BP). The earliest interval of bioturbated mud is deposited rapidly,

allowing the 10 cm sampling interval of HLY03-05GC to resolve a high marine productivity interval between 8,000 and 6,470 ^{14}C yrs BP (8,926–6,050 cal BP).

Several lines of evidence demonstrate an early Holocene climatic optimum in this region with similar timing to HLY03-05GC. Summer melt layers and elevation-corrected $\delta^{18}\text{O}$ temperature reconstructions in the Agassiz Ice Cap ice cores (Fisher et al., 1995; Vinther et al., 2009) demonstrate summer temperatures several degrees warmer than mid-twentieth century between 9,500 and 7,000 years ago. Along West Greenland (65°30' to 68°30'N), range extensions of boreal mollusc species, extinct today in Greenland waters, have been dated to between c. 9,200 and 5,600 cal BP, suggesting summer surface temperature warming of 1–3°C (Funder and Weidick, 1991), and dinoflagellate and foraminiferal data also indicate early Holocene warmth (Levac et al., 2001; Knudsen et al., 2008). On northern Greenland, an area that today has heavy multiyear sea ice cover and landfast ice, wave-generated beach ridge complexes dated to between 8,500 and 6,000 cal BP formed as a result of seasonally open water in a coastal melt zone (Funder and Kjaer, 2007; Polyak et al., 2010). The beach ridge interval coincides with a period of little or no driftwood landings. Driftwood can only land on the coasts of northern Greenland and CAA in environments with multiyear sea ice for transit across the Arctic Ocean and brief periods of ice breakup to bring the driftwood onto land (Funder et al., 2009). On northern Greenland, Möller et al. (2010) reconstruct positive mass balance of local ice caps and northward advances of their outlet glaciers between

8,500–5,500 cal BP. These advances are inferred to be in response to increased precipitation from summer open-water conditions along the North Greenland coast and fjords. England et al. (2008) show abundant drift ice delivery on northern Ellesmere Island landward of the Ward Hunt ice shelf between 9,200 and 5,500 cal BP, indicating that the ice shelf was not present in the early Holocene. In Clements Markham Inlet, which faces the Lincoln Sea on northern Ellesmere Island, drift ice delivery was consistent from 9,900 to 3,500 cal BP, suggesting seasonally open water until then. The first driftwood delivery in Clements Markham Inlet coincides with deposition of the laminated unit in HLY03-05GC. Sea ice algal biomarker IP25, measured in a Holocene sediment core in Barrow Strait, another channel connecting the Arctic Ocean with Baffin Bay, shows consistent sea ice history, with an early Holocene interval of low spring sea ice occurrence between 10,000 and 6,000 cal BP and a moderate increase in spring sea ice between 6,000 and 4,000 cal BP (Vare et al., 2009).

There is strong evidence in the region for Neoglacial cooling beginning between 6,000 and 5,500 cal BP (England et al., 2008; Funder et al., 2009; Vare et al., 2009; Möller et al., 2010; Polyak et al., 2010). Unfortunately, the HLY03-05GC record is not well resolved in this interval because the sedimentation rates are very slow, and the sampling interval was too wide to capture the late Holocene record. However, we surmise that the very slow sedimentation rates and decreases in productivity-indicator benthic foraminifers are consistent with increased sea ice cover and reduced marine productivity in the late Holocene

in Hall Basin (Figure 7). The Neoglacial period is consistently associated with cooling and increased duration and thickness of sea ice cover on northern Greenland and in CAA. On northern Greenland, seasonally open water from 5,500 to 3,000 cal BP allowed driftwood to land after rafting on sea ice, but from 3,000 to 1,000 cal BP, there is very little driftwood indicating more severe sea ice conditions with landfast or multiyear sea ice (Funder et al., 2009). On northern Ellesmere Island, the driftwood record ceases at 5,500 cal BP, documenting the onset of multiyear landfast sea ice and formation of the sea ice shelves, most notably the Ward Hunt Ice Shelf (England et al., 2008). A sharp increase in spring sea ice occurrence was reconstructed beginning by 3,000 cal BP on the basis of IP25 data and biological proxies in several widely spaced sediment cores from CAA (Levac et al., 2001; Knudsen et al., 2008; Vare et al., 2009; Belt et al., 2010).

CONCLUSIONS


Sedimentological and paleoceanographic data from HLY03-05GC indicate that Hall Basin was deglaciated soon before 10,300 cal BP. The core also records ice-distal sedimentation in a glacial bay facing the Arctic Ocean until about 9,000 cal BP. Atlantic Water was present in Hall Basin during deglaciation, suggesting that it may have assisted ice retreat. A transitional unit with high IRD content records the opening of Nares Strait at approximately 9,000 cal BP. High productivity in Hall Basin between 9,000 and 6,000 cal BP reflects reduced sea ice cover as well as throughflow of nutrient-rich Pacific Water. The later Holocene is poorly resolved in the core,

but the slow sedimentation rates and heavier carbon isotope values support an interpretation of increased sea ice cover and decreased productivity during the Neoglacial.

The poor calcium carbonate preservation on the Baffin Island margin has made it challenging to test ideas about the paleoceanographic consequences of the opening of the channels in the Canadian Arctic Archipelago. Few sediment cores have been taken since the

1980s on the Baffin Island shelf where the sedimentation rates are rapid enough to resolve such events. However, given the advances in techniques for studying paleoceanography since the 1980s, it should be possible, with new cores, to gain a better understanding of how the opening of a connection with the Arctic Ocean affected the paleoceanographic development of Baffin Bay and the Labrador Sea.

ACKNOWLEDGEMENTS

We give sincere thanks to François Lapointe (INRS-Centre Eau Terre Environment, Canada) and Natasha Roy (Université Laval, Canada), who are students of Pierre Francus and who made and analyzed the thin sections. Many thanks to Mark Hannon, graduate student at the University of Colorado, Boulder, for making the base map for the study area using the IBCAO database. Bobbi Connard of the College of Oceanic and Atmospheric Sciences (COAS) at Oregon State University graciously coordinated the sampling and x-radiography of the core in 2008. Ursula Quillmann, PhD student in geological sciences at the University of Colorado, Boulder, helped to sample the core at COAS and has helped in many ways on the analyses since then. Sincere thanks go to Svend Funder and an anonymous reviewer for their improvements to the manuscript. This research was supported by NSF OPP 0713755 awarded to Anne E. Jennings, project title: Marine Evidence for GIS Stability and History of Jakobshavn Isbrae, West Greenland, from the LGM to Holocene. 

REFERENCES

- Aagaard, K., and E.C. Carmack. 1989. The role of sea ice and other fresh water in the Arctic circulation. *Journal of Geophysical Research* 94:14,485–14,498, <http://dx.doi.org/10.1029/JC094iC10p14485>.
- Adler, R.E., L. Polyak, J.D. Ortiz, D.S. Kaufman, J.E.T. Channell, C. Xuan, A.G. Grotoli, E. Sellén, and K.A. Crawford. 2009. Sediment record from the western Arctic Ocean with an improved Late Quaternary age resolution: HOTRAX core HLY0503-8JPC, Mendeleev Ridge. *Global and Planetary Change* 68:18–29, <http://dx.doi.org/10.1016/j.gloplacha.2009.03.026>.
- Altenbach, A.V., T. Heeger, P. Linke, M. Spindler, and A. Thies. 1993. *Miliolinella subrotunda* (Montagu), a miliolid foraminifer building large detritic tubes for

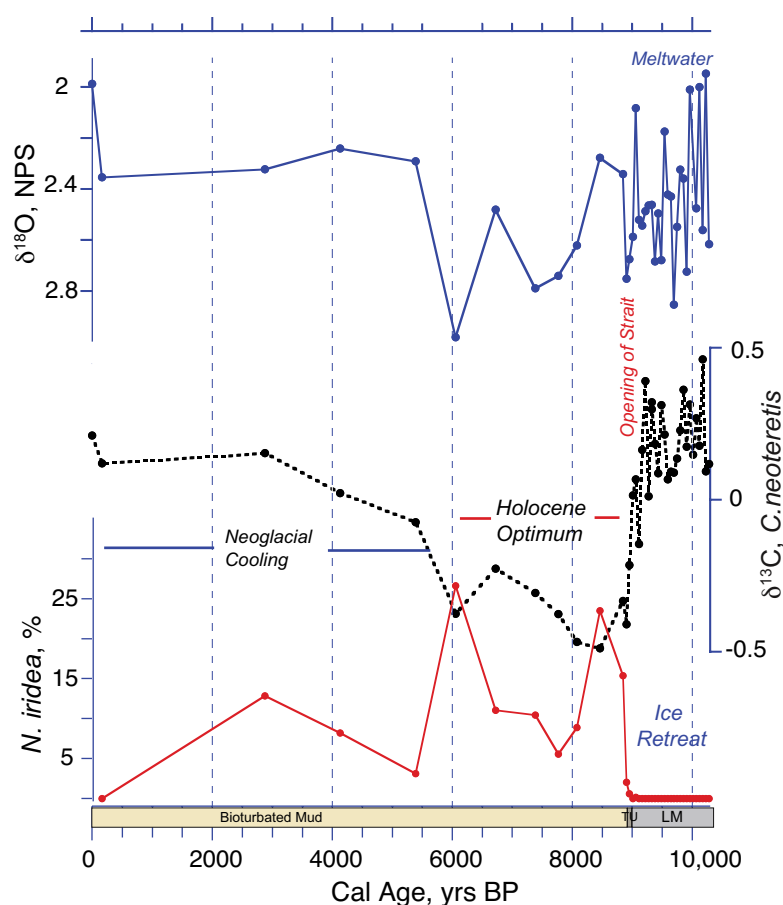


Figure 7. Key paleoceanographic proxies shown against calibrated age in HLY03-05GC. $\delta^{18}\text{O}$ NPS in the laminated mud supports glacial meltwater entering the Hall Basin from the retreating ice sheets. The Holocene Optimum is recorded by evidence of high marine productivity (*N. iridea* % and light $\delta^{13}\text{C}$ *C. neoteretis*). Low sedimentation rates in the upper bioturbated mud precluded high-resolution evaluation of Neoglacial cooling, but the evidence shown is consistent with cooling after 6,000 cal yrs BP.

- a temporary epibenthic lifestyle. *Marine Micropaleontology* 20:293–301, [http://dx.doi.org/10.1016/0377-8398\(93\)90038-Y](http://dx.doi.org/10.1016/0377-8398(93)90038-Y).
- Andrews, J.T., and G. Dunhill. 2004. Early to mid-Holocene Atlantic water influx and deglacial meltwater events, Beaufort Sea slope, Arctic Ocean. *Quaternary Research* 61:14–21, <http://dx.doi.org/10.1016/j.yqres.2003.08.003>.
- Azetsu-Scott, K., A. Clarke, K. Falkner, J. Hamilton, E.P. Jones, C. Lee, B. Petrie, S. Prinsenberg, M. Starr, and P. Yeats. 2010. Calcium carbonate saturation states in the waters of the Canadian Arctic Archipelago and the Labrador Sea. *Journal of Geophysical Research* 115, C11021, <http://dx.doi.org/10.1029/2009JC005917>.
- Belt, S.T., L.L. Vare, G. Masse, H.R. Manners, J.C. Price, S.E. MacLachlan, J.T. Andrews, and S. Schmidt. 2010. Striking similarities in temporal changes to spring sea ice occurrence across the central Canadian Arctic Archipelago over the last 7000 years. *Quaternary Science Reviews* 29:3,489–3,504, <http://dx.doi.org/10.1016/j.quascirev.2010.06.041>.
- Berger, A., and M.F. Loutre. 1991. Insolation values for the climate of the last 10 million years. *Quaternary Science Reviews* 10:297–317, [http://dx.doi.org/10.1016/0277-3791\(91\)90033-Q](http://dx.doi.org/10.1016/0277-3791(91)90033-Q).
- Blake, W. Jr. 1970. Studies of glacial history in Arctic Canada. *Canadian Journal of Earth Sciences* 7:634–664, <http://dx.doi.org/10.1139/e70-065>.
- Coulthard, R.D., M.F.A. Furze, A.J. Pienkowski, F.C. Nixon, and J.H. England. 2010. New marine DR values for Arctic Canada. *Quaternary Geochronology* 5:419–434, <http://dx.doi.org/10.1016/j.quageo.2010.03.002>.
- Cuven, S., P. Francus, and S. Lamoureux. 2010. Estimation of grain size variability with micro X-ray fluorescence in laminated lacustrine sediments, Cape Bounty, Canadian High Arctic. *Journal of Paleolimnology* 44:803–817, <http://dx.doi.org/10.1007/s10933-010-9453-1>.
- Dyke, A.S., J.E. Dale, and R.N. McNeely. 1996. Marine molluscs as indicators of environmental change in glaciated North America and Greenland during the last 18,000 years. *Geographie Physique et Quaternaire* 50:125–184.
- Dyke, A.S., J.T. Andrews, P.U. Clark, J.H. England, G.H. Miller, J. Shaw, and J.J. Veillette. 2002. The Laurentide and Innuitian Ice Sheet during the Last Glacial Maximum. *Quaternary Science Reviews* 21:9–31, [http://dx.doi.org/10.1016/S0277-3791\(01\)00095-6](http://dx.doi.org/10.1016/S0277-3791(01)00095-6).
- Dyke, A.S., R. McNeely, J. Southon, J.T. Andrews, W.R. Peltier, J.J. Clague, J.H. England, J.-M. Gagnon, and A. Baldinger. 2003. Preliminary assessment of Canadian marine reservoir ages. P. A 23 in *Program and Abstracts, Canadian Quaternary Association–Canadian Geomorphological Research Group Joint Meeting, Halifax*.
- England, J. 1999. Coalescent Greenland and Innuitian ice during the Last Glacial Maximum: Revising the Quaternary of the Canadian High Arctic. *Quaternary Science Reviews* 18:421–426, [http://dx.doi.org/10.1016/S0277-3791\(98\)00070-5](http://dx.doi.org/10.1016/S0277-3791(98)00070-5).
- England, J.H., N. Atkinson, J.B. Bednarski, A.S. Dyke, D.A. Hodgson, and C. Ó Cofaigh. 2006. The Innuitian Ice Sheet: Configuration, dynamics and chronology. *Quaternary Science Reviews* 25:689–703, <http://dx.doi.org/10.1016/j.quascirev.2005.08.007>.
- England, J.H., T.R. Lakeman, D.S. Lemmen, J.M. Bednarski, T.G. Stewart, and D.J.A. Evans. 2008. A millennial-scale record of Arctic Ocean sea ice variability and the demise of the Ellesmere Island ice shelves. *Geophysical Research Letters* 35, L19502, <http://dx.doi.org/10.1029/2008GL034470>.
- Fairbanks, R.G. 1989. A 17,000-year glacio-eustatic sea level record: Influence of glacial melting rates on the Younger Dryas event and deep-ocean circulation. *Nature* 342:637–642, <http://dx.doi.org/10.1038/342637a0>.
- Falkner, K. 2003. *Research Cruise Report Hly031: Mission Conducted Aboard USCGC Healy in Northern Baffin Bay and Nares Strait. Variability and Forcing of Fluxes Through Nares Strait and Jones Sound: A Freshwater Emphasis*. US National Science Foundation, Office of Polar Programs, Arctic Division. 128 pp.
- Fisher, D.A., R.M. Koerner, and N. Reeh. 1995. Holocene climatic records from Agassiz ice cap, Ellesmere Island, NWT, Canada. *The Holocene* 5:19–24, <http://dx.doi.org/10.1177/095968369500500103>.
- Francus, P., and C.A. Asikainen. 2001. Sub-sampling unconsolidated sediments: A solution for the preparation of undisturbed thin-sections from clay-rich sediments. *Journal of Paleolimnology* 26:323–326, <http://dx.doi.org/10.1023/A:1017572602692>.
- Funder, S. 1989. Introduction: Quaternary geology of the ice-free areas and adjacent shelves of Greenland. Chapter 13 in *Quaternary Geology of Canada and Greenland*. R.J. Fulton, ed., Geological Survey of Canada, Geology of Canada, no. 1 (also Geological Society of America, The Geology of North America, v. K-1).
- Funder, S., and L. Hansen. 1996. The Greenland Ice Sheet: A model for its culmination and decay during and after the last glacial maximum. *Bulletin of the Geological Society of Denmark* 42:137–152.
- Funder, S., and K. Kjær. 2007. Ice free Arctic Ocean, an early Holocene analogue. *Eos, Transactions, American Geophysical Union* 88(52), Fall Meeting Supplement, Abstract PP11A-0203.
- Funder, S., K. Kjær, H. Linderson, and J. Olsen. 2009. Arctic driftwood: An indicator of multiyear sea ice and transportation routes in the Holocene. *Geophysical Research Abstracts* 11:EGU2009-13045.
- Funder, S., K. Kjellerup, K. Kjær, and C. Ó Cofaigh. In press. The Greenland Ice Sheet, the last 300,000 years: A review. In *Quaternary Glaciations, Extent and Chronology. Part IV. A Closer Look*. Developments in Quaternary Science 16. Elsevier, Amsterdam.
- Funder, S., and A. Weidick. 1991. Holocene boreal molluscs in Greenland: Palaeoceanographic implications. *Palaeogeography, Palaeoclimatology, Palaeoecology* 85:123–135, [http://dx.doi.org/10.1016/0031-0182\(91\)90029-Q](http://dx.doi.org/10.1016/0031-0182(91)90029-Q).
- Gooday, A.J., and J.A. Hughes. 2002. Foraminifera associated with phytodetritus deposits at a bathyal site in the northern Rockall Trough (NE Atlantic): Seasonal contrasts and a comparison of stained and dead assemblages. *Marine Micropaleontology* 46:83–110, [http://dx.doi.org/10.1016/S0377-8398\(02\)00050-6](http://dx.doi.org/10.1016/S0377-8398(02)00050-6).
- Goosse, H., E. Driesschaert, T. Fichefet, and M.-F. Loutre. 2007. Information on the early Holocene climate constrains the summer sea ice projections for the 21st century. *Climate of the Past Discussions* 2:999–1,020.
- Hald, M., and S. Korsun. 1997. Distribution of modern benthic foraminifera from fjords of Svalbard, European Arctic. *Journal of Foraminiferal Research* 27:101–122, <http://dx.doi.org/10.2113/gsjfr.27.2.101>.
- Hald, M., P.I. Steinsund, T. Dokken, S. Korsun, L. Polyak, and R. Aspeli. 1994. Recent and Late Quaternary distribution of *Elphidium excavatum* f. *clavata* in Arctic Seas. *Cushman Foundation Special Publication* 32:141–153.
- Holland, D.M., R.H. Thomas, B. DeYoung, M.H. Ribergaard, and B. Lyberth. 2008. Acceleration of Jakobshavn Isbrae triggered by warm subsurface ocean waters. *Nature Geoscience* 1:659–664, <http://dx.doi.org/10.1038/ngeo316>.
- Hughen, K.A., M.G.L. Baillie, E. Bard, A. Bayliss, J.W. Beck, C.J.H. Bertrand, P.G. Blackwell, C.E. Buck, G.S. Burr, K.B. Cutler, and others. 2004. Marine04 marine radiocarbon age calibration, 26–0 ka BP. *Radiocarbon* 46:1,059–1,086.
- Jakobsson, M., R. Macnab, L. Mayer, R. Anderson, M. Edwards, J. Hatzky, H.-W. Schenke, and P. Johnson. 2008. An improved bathymetric portrayal of the Arctic Ocean: Implications for ocean modeling and geological, geophysical and oceanographic analyses. *Geophysical Research Letters* 35, L07602, <http://dx.doi.org/10.1029/2008GL033520>.
- Jakobsson, M., J. Nilsson, M.A. O'Regan, J. Backman, L. Löwemark, J.A. Dowdeswell, F. Colleoni, C. Marcussen, L. Anderson, G. Björck, and others. 2010. An Arctic Ocean ice shelf during MIS 6 constrained by new geophysical and geological data. *Quaternary Science Reviews* 29:3,505–3,517, <http://dx.doi.org/10.1016/j.quascirev.2010.03.015>.
- Jennings, A.E., and G. Helgadottir. 1994. Foraminiferal assemblages from the fjords and shelf of Eastern Greenland. *Journal of Foraminiferal Research* 24:123–144, <http://dx.doi.org/10.2113/gsjfr.24.2.123>.

- Jennings, A.E., N.J. Weiner, G. Helgadottir, and J.T. Andrews. 2004. Modern foraminiferal faunas of the southwestern to northern Iceland shelf: Oceanographic and environmental controls. *Journal of Foraminiferal Research* 34:180–207, <http://dx.doi.org/10.2113/34.3.180>.
- Johnson, H.L., A. Münchow, K.K. Falkner, and H. Melling. 2011. Ocean circulation and properties in Petermann Fjord, Greenland. *Journal of Geophysical Research* 116, C01003, <http://dx.doi.org/10.1029/2010JC006519>.
- Jones, E.P., J.H. Swift, L.G. Anderson, M. Lipizer, G. Civitarese, K.K. Falkner, G. Kattner, and F. McLaughlin. 2003. Tracing Pacific water in the North Atlantic Ocean. *Journal of Geophysical Research* 108, 3116, <http://dx.doi.org/10.1029/2001JC001141>.
- Kelly, M., and O. Bennike. 1992. *Quaternary Geology of Western and Central North Greenland*. Rapport Grønlands Geologiske Undersøgelse 153, GGU, Copenhagen, 34 pp.
- Knudsen, K.L., B. Stabell, M.-S. Seidenkrantz, J. Eiriksson, and W. Blake Jr. 2008. Deglacial and Holocene conditions in northernmost Baffin Bay: Sediments, foraminifera, diatoms and stable isotopes. *Boreas* 37:346–376, <http://dx.doi.org/10.1111/j.1502-3885.2008.00035.x>.
- Kwok, R. 2005. Variability of Nares Strait ice flux. *Geophysical Research Letters* 32, L24502, <http://dx.doi.org/10.1029/2005GL024768>.
- Larsen, N.K., K.H. Kjær, S. Funder, P. Möller, H.C. Linge, A. Schomacker, J. van der Meer, and D. Darby. 2010. Late Quaternary glaciation history of northernmost Greenland: Evidence of shelf-based ice. *Quaternary Science Reviews* 29:3,399–3,414, <http://dx.doi.org/10.1016/j.quascirev.2010.07.027>.
- Levac, E., A. de Vernal, and W. Blake Jr. 2001. Sea-surface conditions in the northernmost Baffin Bay during the Holocene: Palynological evidence. *Journal of Quaternary Science* 16:353–363, <http://dx.doi.org/10.1002/jqs.614>.
- Mackensen, A., H.W. Hubberten, T. Bickert, G. Fischer, and D.K. Fütterer. 1993. The $\delta^{13}\text{C}$ in benthic foraminifera tests of *Fontbotia wuellerstorfi* relative to the $\delta^{13}\text{C}$ of dissolved inorganic carbon in Southern Ocean Deep Water: Implications for ocean circulation models. *Paleoceanography* 5:161–185, <http://dx.doi.org/10.1029/93PA01291>.
- Maslin, M.A., and G.E.A. Swann. 2005. Isotopes in marine sediments. Pp. 227–290 in *Isotopes in Palaeoenvironmental Research*. M.J. Leng, ed., Springer Verlag, Dordrecht, The Netherlands.
- Melling, H., Y. Gratton, and G. Ingram. 2001. Ocean circulation within the North Water polynya of Baffin Bay. *Atmosphere-Ocean* 39(3):301–325, <http://dx.doi.org/10.1080/07055900.2001.9649683>.
- Möller, P., N.K. Larsen, K.H. Kjær, S. Funder, A. Schomacker, H. Linge, and D. Fabel. 2010. Early to middle Holocene valley glaciations on northernmost Greenland. *Quaternary Science Reviews* 29:3,379–3,398, <http://dx.doi.org/10.1016/j.quascirev.2010.06.044>.
- Mudie, P.J., A. Rochon, M.A. Prins, D. Soenarjo, S.R. Troelstra, E. Levac, D.B. Scott, L. Roncaglia, and A. Kuijpers. 2006. Late Pleistocene–Holocene marine geology of Nares Strait region: Palaeoceanography from foraminifera and dinoflagellate cysts, sedimentology and stable isotopes. *Polarforschung* 74:169–183.
- Münchow, A., K.K. Falkner, and H. Melling. 2007. Spatial continuity of measured seawater and tracer fluxes through Nares Strait, a dynamically wide channel bordering the Canadian Archipelago. *Journal of Marine Research* 65:759–788, <http://dx.doi.org/10.1357/002224007784219048>.
- Münchow, A., H. Melling, K.K. Falkner. 2006. An observational estimate of volume and freshwater flux leaving the Arctic Ocean through Nares Strait. *Journal of Physical Oceanography* 36:2,025–2,041, <http://dx.doi.org/10.1175/JPO2962.1>.
- Ó Cofaigh, C., and J.A. Dowdeswell. 2001. Laminated sediments in glacial marine environments: Diagnostic criteria for their interpretation. *Quaternary Science Reviews* 20:1,411–1,436, [http://dx.doi.org/10.1016/S0277-3791\(00\)00177-3](http://dx.doi.org/10.1016/S0277-3791(00)00177-3).
- Osterman, L.E., R.Z. Poore, and K.M. Foley. 1999. *Distribution of Benthic Foraminifers (> 125 μm) in the Surface Sediments of the Arctic Ocean*. US Geological Survey Bulletin 2164. 28 pp.
- Parnell, J., S. Bowden, J.T. Andrews, and C. Taylor. 2007. Biomarker determination as a provenance tool for detrital carbonate events (Heinrich events?): Fingerprinting Quaternary glacial sources into Baffin Bay. *Earth and Planetary Science Letters*, <http://dx.doi.org/10.1016/j.epsl.2007.02.021>.
- Pickering, K.T., D.A.V. Stow, M.P. Watson, and R.N. Hiscott. 1986. Deep-water facies, processes and models: A review and classification scheme for modern and ancient sediments. *Earth-Science Reviews* 23:75–174, [http://dx.doi.org/10.1016/0012-8252\(86\)90001-2](http://dx.doi.org/10.1016/0012-8252(86)90001-2).
- Polyak, L., R.B. Alley, J.T. Andrews, J. Brigham-Grette, T.M. Cronin, D.A. Darby, A.S. Dyke, J.J. Fitzpatrick, S. Funder, M. Holland, and others. 2010. History of sea ice in the Arctic. *Quaternary Science Reviews* 29:1,757–1,778, <http://dx.doi.org/10.1016/j.quascirev.2010.02.010>.
- Polyak, L., S. Korsun, L.A. Febo, V. Stanovoy, T. Khuisid, M. Hald, B.E. Paulsen, D.J. Lubinski. 2002. Benthic foraminiferal assemblages from the southern Kara Sea, a river-influenced Arctic marine environment. *Journal of Foraminiferal Research* 32:252–273, <http://dx.doi.org/10.2113/32.3.252>.
- Reimer, P.J., M.G.L. Baillie, E. Bard, A. Bayliss, J.W. Beck, P.G. Blackwell, C. Bronk-Ramsey, C.E. Buck, G.S. Burr, R.L. Edwards, and others. 2009. IntCal09 and Marine09 radiocarbon age calibration curves, 0–50,000 years cal BP. *Radiocarbon* 51:1,111–1,150.
- Rytter, F., K.L. Knudsen, M.-S. Seidenkrantz, and J. Eiriksson. 2002. Distribution of benthic foraminifera on the North Icelandic shelf and slope. *Journal of Foraminiferal Research* 32:217–245, <http://dx.doi.org/10.2113/32.3.217>.
- Sadler, H.E. 1976. Water, heat and salt transports through Nares Strait, Ellesmere Island. *Journal of Fisheries Research Board of Canada* 33:2,286–2,295.
- Samelson, R.M., T. Agnew, H. Melling, A. Münchow. 2006. Evidence for atmospheric control of sea-ice motion through Nares Strait. *Geophysical Research Letters* 33, L02506, <http://dx.doi.org/10.1029/2005GL025016>.
- Steinsund, P.-I. 1994. Benthic foraminifera in surface sediments of the Barents and Kara Seas: Modern and late Quaternary applications. Dr. Scient. Thesis, University of Tromsø.
- Stuiver, M., and P.J. Reimer. 1993. Extended ^{14}C database and revised CALIB radiocarbon calibration program. *Radiocarbon* 35:215–230.
- Stuiver, M., P.J. Reimer, and R.W. Reimer. 2010. CALIB 6.0. Available online at: <http://calib.qub.ac.uk/calib> (accessed June 24, 2011).
- Syvitski, J.P.M., and F.J. Hein. 1991. *Sedimentology of an Arctic Basin: Itirbilung Fiord, Baffin Island, Northwest Territories*. Paper 91-11, Geological Survey of Canada, Ottawa, Ontario, 66 pp.
- Tang, C.C.L., C.K. Ross, T. Yao, B. Petrie, B.M. DeTracey, and E. Dunlap. 2004. The circulation, water masses and sea-ice of Baffin Bay. *Progress in Oceanography* 63:183–228, <http://dx.doi.org/10.1016/j.pocean.2004.09.005>.
- Vare, L.L., G. Massé, T.R. Gregory, C.W. Smart, and S.T. Belt. 2009. Sea ice variations in the central Canadian Arctic Archipelago during the Holocene. *Quaternary Science Reviews* 28:1,354–1,366, <http://dx.doi.org/10.1016/j.quascirev.2009.01.013>.
- Vinther, B.M., S.L. Buchardt, H.B. Clausen, D. Dahl-Jensen, S.J. Johnsen, D.A. Fisher, R.M. Koerner, D. Raynaud, V. Lipenkov, K.K. Andersen, and others. 2009. Holocene thinning of the Greenland Ice Sheet. *Nature* 461:385–388, <http://dx.doi.org/10.1038/nature08355>.
- Wetzel, A. 1991. Ecologic interpretation of deep-sea trace fossil communities. *Palaeogeography, Palaeoclimatology, Palaeoecology* 85:47–69, [http://dx.doi.org/10.1016/0031-0182\(91\)90025-M](http://dx.doi.org/10.1016/0031-0182(91)90025-M).
- Zreda, M., J. England, F. Phillips, D. Elmore, and P. Sharma. 1999. Unblocking of the Nares Strait by Greenland and Ellesmere Ice-Sheet retreat 10,000 years ago. *Nature* 398:139–142, <http://dx.doi.org/10.1038/18197>.